International Journal of Research
Available at https://edupediapublications.org/journals
p-ISSN: 2348-6848
e-ISSN: 2348-795X
Volume 03 Issue 13
September 2016

Closed loop control of High Step-Up DC-DC Converter for Hybrid Switched-Inductor Converters

V Jyothsna
M-tech Student Scholar
Department of Electrical & Electronics Engineering,
Loyola Institute of Technology and Management,Dhullipalla,
Guntur (Dt); A.P, India.

P Nalini
Assistant Professor
Department of Electrical & Electronics Engineering,
Loyola Institute of Technology and Management,Dhullipalla,
Guntur (Dt); A.P, India.

Abstract - This paper proposes a high voltage gain dc/dc converter with coupled inductor cells and switched capacitor for renewable energy applications. It includes coupled inductor, switched capacitor and voltage multiplier cell. Switched capacitor charged during off period by using the energy stored in the coupled inductor. This will increase the performance of the converter. The voltage gain of traditional boost converter is limited, considering the issues such as the system efficiency and current ripple. First, the topological derivation of H-SLCs is deduced by combining the passive and active switched inductor unit; second, this paper illustrates the operation modes of the proposed asymmetrical and symmetrical converters; third, the performance of the proposed converters is analyzed in detail and compared with existing converters. In this paper, a new H-SLCS step up converter with closed loop control is proposed, It is analyzed, designed, simulated with MATLAB Simulink. Conventional DC-DC boost converters are not able to provide high step-up voltage gains. This paper presents transformerless dc-dc converters with closed loop control to achieve high step-up voltage gain without an extremely high duty ratio. Moreover closed loop control methodology is used for voltage drift problems.

Index Terms—DC/DC converter, high step-up, switchedinductor.

I. INTRODUCTION

Reliability becomes more important to power supplies for industrial applications. So, power supplies have adopted a battery back-up system in several applications. In addition to that, renewable energy such as the fuel cell is a hot issue in the research field. The common power supply for the above applications is a high boost converter to step up the low input voltage to high output voltage [1]. DC–DC converter with a high step-up voltage gain is used for many applications, such as high-intensity discharge lamp ballasts for automobile headlamps, fuel-cell energy conversion systems, solar-cell energy conversion systems, front-end stage for a battery source, and telecommunication industry and battery backup systems for uninterruptible power supplies [2].

Theoretically, a dc–dc boost converter can achieve a high step up voltage gain with an extremely high duty ratio. However, in practice, the step-up voltage gain is limited due to the effect of power switches, rectifier diodes, and the equivalent series resistance (ESR) of inductors and capacitors. Moreover, the extremely high duty-ratio operation will result in a serious reverse-recovery problem. A dc–dc fly back converter is a very simple structure with a high step-up voltage gain and an electrical isolation, but the active switch of this converter will suffer a high voltage stress due to the leakage inductance of the transformer [3-5]. For recycling the energy of the leakage inductance and minimizing the voltage stress on the active switch, some energy-regeneration techniques have been proposed to clamp the voltage stress on the active switch and to recycle the leakage-inductance energy. The coupled-inductor techniques provide solutions to achieve a high voltage gain, a low voltage stress on the active switch, and a high efficiency without the penalty of high duty ratio [6-7].

Converters with charge pump will provide voltage gain in proportion to the stage number of capacitors, but its drawback includes fixed voltage gain and large device area. In [8] diode capacitor techniques are implemented. It can achieve high voltage gin in proportional to the number of stages, which is able to be extended by adding capacitors and diodes. But it may result in the larger voltage drop consumption due to cut in voltage of the diodes in series.

Tapped inductor technology is explained in [9]. Different converter topologies are explained. Coupled inductor based converters also achieve high step-up voltage gain by adjusting the turns ratio [10]. However the stored energy in the leakage inductor causes a voltage spike on the main switch and deteriorates the conversion efficiency. To overcome this problem, coupled inductor based converter with active clamping circuits are presented [11].It compare proposed converter and conventional boost converter with coupled inductor only and active clamp circuit only. High step-up converter with two switch [12] and one switch are explained. As no of switches increased losses will increased. However the conversion ratio is not large enough.

In order to achieve high voltage gain, this paper proposes a high step-up voltage gain dc/dc converter with coupled inductor and switched capacitor techniques. Here Pulse Width Modulation techniques are introduced to get better voltage regulation [13].

The double stage power electronics interface for photovoltaic and fuel cell systems in residential and general grid-connected applications is commonly based on a boosting converter that feeds an inverter. This is due

International Journal of Research
Available at https://edupediapublications.org/journals
p-ISSN: 2348-6848
e-ISSN: 2348-795X
Volume 03 Issue 13
September 2016

to the requirement of increasing the voltage given by the source to the grid-connected inverter operating conditions. The most commonly used dc/dc converter in the first stage of this grid-connection and residential systems is a boost converter which provides an acceptable voltage conversion ratio and also requests a continuous current from the power source. Similarly, in vehicular and stand-alone applications the boost converter is also widely adopted [14].

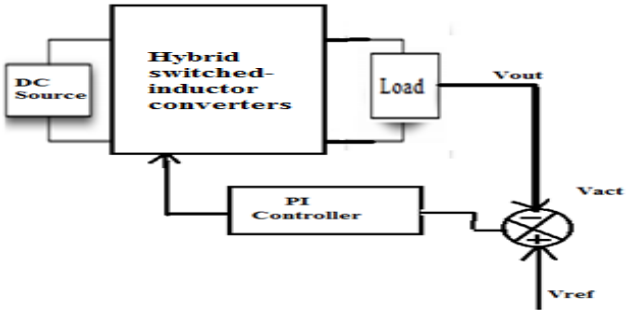

Figure 1. Block Diagram of Hybrid Switched Inductor Converter with Closed Loop Controller.

II. TOPOLOGICAL DERIVATION OF THE H-SLC

Transformerless high-gain converters with passive switchedinductor (P-SL) unit and active switched-inductor (A-SL) unit have been presented, respectively, as shown in Fig. 2. The P-SL unit consists two inductors L1, L2 and three diodes D1, D2, D3, when the potential voltage across the point A and B (i.e., VAB) is positive, D1, D2 become conduct and D3 is shutting off, two inductors are parallel connected; when VAB becomes negative, D1, D2 are reverse biased and D3 is conducted, then, the two inductors are series connected with the input (1-1') of the two-port network.

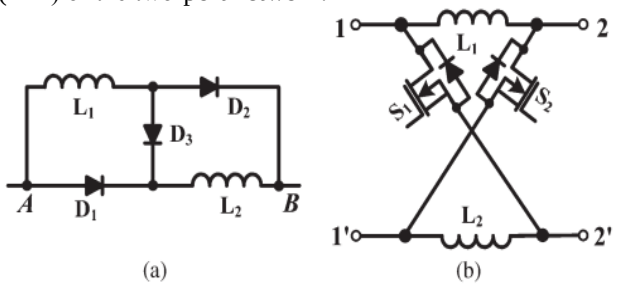

Fig. 2. Switched-inductor unit. (a) P-SL. (b) A-SL.

The A-SL unit is made up of two switches S1, S2 and two inductors L1, L2, the working principle of A-SL is similar to that of P-SL, when the switches S1 and S2 are turned on simultaneously, the inductors L1 and L2 are parallel connected; when S1 and S2 are turned off, L1 and L2 are series connected. A high voltage gain can be achieved by combining the PSL and A-SL units. The inductors L1 and L2 in A-SL unit can be substituted with P-SL unit, then the proposed H-SLCs can be obtained, as shown in Fig. 3, where Fig. 3(a) shows the asymmetrical structure, and Fig. 3(b) shows the symmetrical structure. The power switches share the same switching signals, which is easy to control. When the switches are conduct, the inductors operates in parallel connection and charged by the

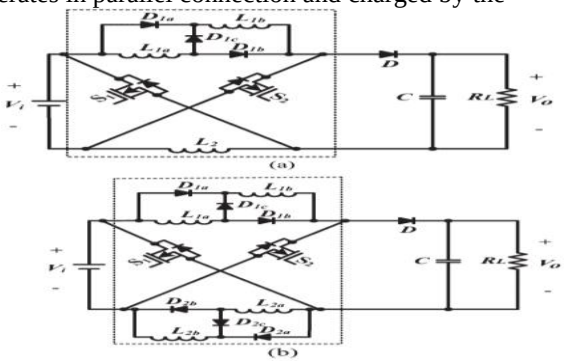

Fig. 3. Proposed H-SLC. (a) Asymmetrical structure. (b) Symmetrical structure.

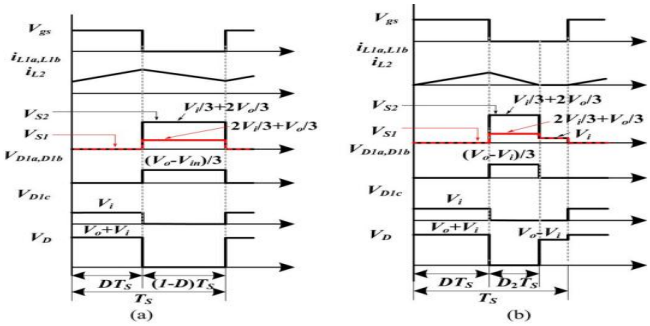

Fig. 4. Key waveforms of AH-SLC. (a) CCM. (b) DCM.

power source; when the switches are shutting off, the inductors operates in series connection and discharged to the output.

III. OPERATION PRINCIPLE OF PROPOSED CONVERTERS

A. Operating Modes of Asymmetrical Structure with an Equal Inductance

Fig. 4 illustrates the key waveforms of the proposed asymmetrical H-SLC (AH-SLC) in continuous-conduction mode

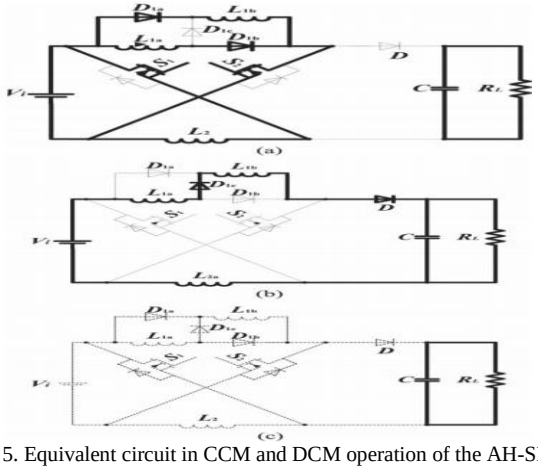

Fig. 5. Equivalent circuit in CCM and DCM operation of the AH-SLC.

(CCM) operation and discontinuous-conduction mode (DCM) operation. The equivalent circuit in CCM operation is shown in Fig. 5(a) and (b).

International Journal of Research
Available at https://edupediapublications.org/journals
p-ISSN: 2348-6848
e-ISSN: 2348-795X
Volume 03 Issue 13
September 2016

1) Mode 1 [t0 − t1]: The switches S1 and S2 are turned on during this time interval. The equivalent circuit is shown in Fig. 5(a). The three inductors L1a, L1b, L2 are charged in parallel by the power source. The voltage across the inductors can be expressed as

$$V_{L1a} = V_{L1b} = V_{L2} = V_i \quad (1)$$

2) Mode 2 [t1 − t2]: During this time interval, S1 and S2 are turned off. The equivalent circuit is shown in Fig. 5(b).

The three inductors L1a, L1b, L2 are series connected to transfer the energy to output. The voltage across the inductors is

$$V_{L1a} = V_{L1b} = V_{L2} = \frac{V_i - V_o}{3} \quad (2)$$

Based on the voltage–second balancing of inductors, the following equation can be derived:

$$D \cdot V_i + (1 - D) \cdot \frac{V_i - V_o}{3} = 0 \quad (3)$$

The voltage gain in CCM operation is

$$G_{\mathrm{CCM}} = \frac{V_o}{V_i} = \frac{1 + 2D}{1 - D} \quad (4)$$

The equivalent circuit in DCM operation is shown in Fig. 5(a)–(c).

1) Mode 1 [t0 − t1]: This mode is similar to Mode 1 in CCM operation. During the time t1, the peak current through the inductors L1a, L1b, L2 is

$$i_{L1ap} = i_{L1bp} = i_{L2a} = \frac{V_i}{L} D T_S \quad (5)$$

Where L1a = L1b = L2 = L.

2) Mode 2 [t1 − t2]: This mode is similar to Mode 2 in CCM operation. During time t2, the inductor current decreased to 0. iL1ap, iL1bp, iL2a can be expressed as

$$i_{L1ap} = i_{L1bp} = i_{L2a} = \frac{V_o - V_i}{3L} D_2 T_S \quad (6)$$

3) Mode 3 [t2 − t3]: During this time interval, the equivalent circuit is shown in Fig. 5(c). The load is supplied by the capacitor. Combining (5) and (6), the relationship between D2 and D is

$$D_2 = \frac{3V_i}{V_o - V_i} D \quad (7)$$

The average current through the output diode is equal to load current Io; therefore,

$$\frac{1}{2} D_2 i_{L1p} = I_o = \frac{V_o}{R_L} \quad (8)$$

Combining (5), (7), and (8), we can derive

$$V_o = \frac{1 + \sqrt{1 + \frac{6D^2}{\tau}}}{2} V_i \quad (9)$$

The time constant τ is defined as

$$\tau = \frac{L f_S}{R_L} \quad (10)$$

Where L is the inductance of the three inductors; fS is the switching frequency; RL is the load. The voltage gain in DCM operation is

$$G_{\mathrm{DCM}} = \frac{V_o}{V_i} = \frac{1 + \sqrt{1 + \frac{6D^2}{\tau}}}{2} \quad (11)$$

B. Operating Modes of Symmetrical Structure with an Equal Inductance

Fig. 6 shows the key waveforms of the proposed symmetrical H-SLC (SH-SLC) in CCM operation and DCM operation. The equivalent circuit in CCM operation is shown in Fig. 7(a) and (b).

1) Mode 1 [t0 − t1]: During this time interval, S1 and S2 areturned on. The current-flow path is shown in Fig. 7(a).The four inductors L1a, L1b, L2a, L2b are charged by the

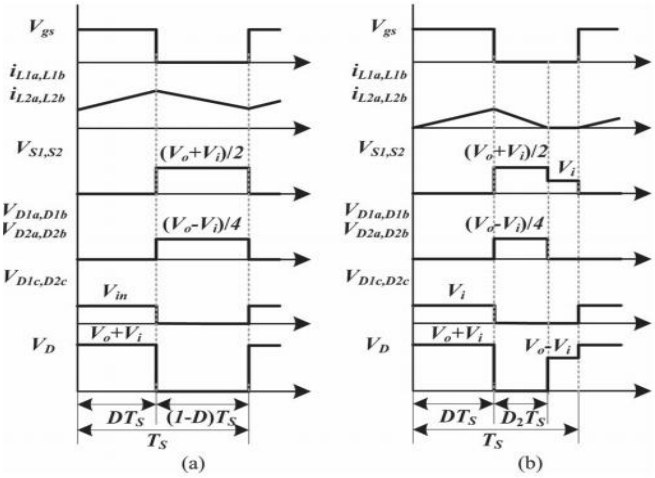

Fig. 6. Key waveforms of SH-SLC. (a) CCM. (b) DCM.

power source in parallel. The voltage across the inductors can be expressed as

$$V_{L1a} = V_{L1b} = V_{L2a} = V_{L2b} = V_i \quad (12)$$

2) Mode 2 [t1 − t2]: During this time interval, S1 and S2 are turned off. The current-flow path is shown in Fig. 7(b). The four inductors L1a, L1b, L2a, L2b are discharged to the output in series. The voltage across the inductors is

$$V_{L1a} = V_{L1b} = V_{L2a} = V_{L2b} = \frac{V_i - V_o}{4} \quad (13)$$

International Journal of Research
Available at https://edupediapublications.org/journals
p-ISSN: 2348-6848
e-ISSN: 2348-795X
Volume 03 Issue 13
September 2016

Based on the voltage–second balancing of inductors, we canderive

$$D \cdot V_i + (1-D) \cdot \frac{V_i - V_o}{4} = 0 \quad (14)$$

The voltage gain in CCM operation is

$$G_{CCM} = \frac{V_o}{V_i} = \frac{1+3D}{1-D} \quad (15)$$

The equivalent circuit in DCM operation is shown in Fig. 7(a)–(c).

1) Mode 1 [t0 − t1]: This mode is similar to Mode 1 in CCM operation. During time t1, the peak current iL through the inductors L1a, L1b, L2a, L2b is

$$i_{L1ap} = i_{L1bp} = i_{L2ap} = i_{L2bp} = \frac{V_i}{L} DT_S \quad (16)$$

Where L1a = L1b = L2a = L2b = L.

2) Mode 2 [t1 − t2]: This mode is similar to Mode 2 in CCM operation. During time t2, the inductor current decreased to 0. iL1ap, iL1bp, iL2ap, iL2bp can be expressed as

$$i_{L1ap} = i_{L1bp} = i_{L2ap} = i_{L2bp} = \frac{V_o - V_i}{4L} D_2 T_S \quad (17)$$

3)Mode 3 [t2 − t3]: During this time interval, the equivalent circuit is shown in Fig. 5(c). The load is supplied by

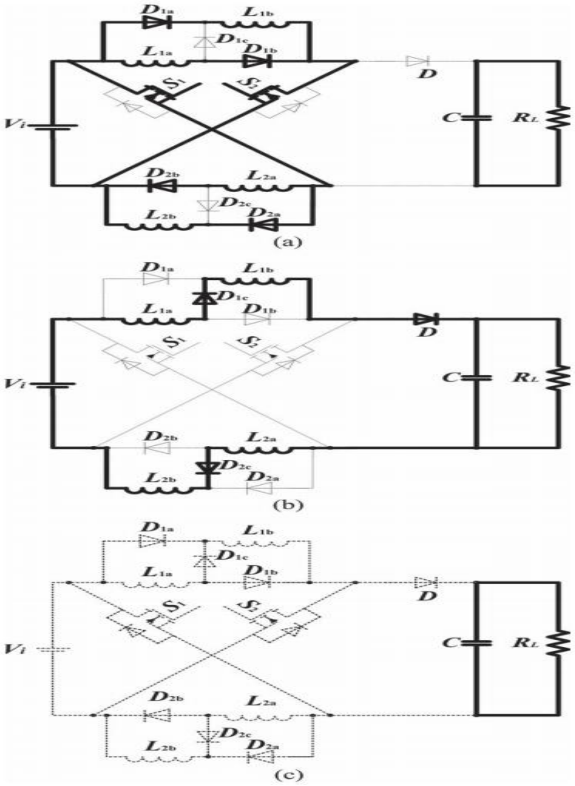

Fig. 7. Equivalent circuit of SH-SLC in CCM and DCM.

The capacitor. Combining (16) and (17), D2 could be expressed as

$$D_2 = \frac{4V_i}{V_o - V_i} D \quad (18)$$

The average current through the output diode is equal to load current Io; therefore,

$$\frac{1}{2} D_2 i_{L1p} = I_o = \frac{V_o}{R_L} \quad (19)$$

Combining (16), (18) and (19), the output voltage can beobtained

$$V_o = \left(\frac{1}{2} + \frac{1}{2} \sqrt{1 + \frac{8D^2}{\tau}} \right) V_i \quad (20)$$

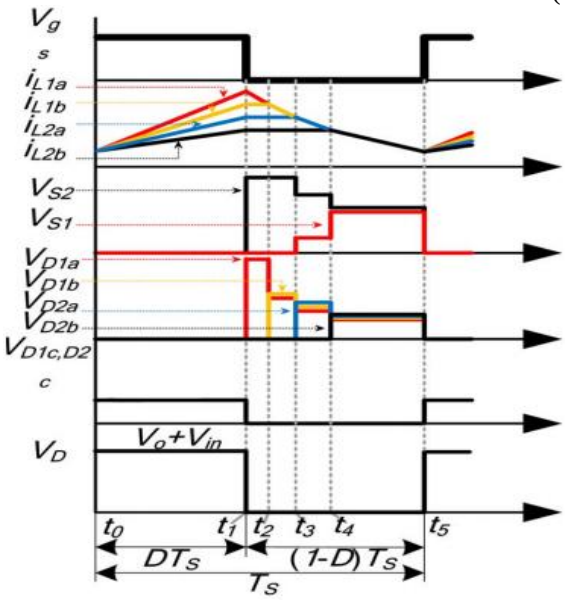

Fig. 8. Key waveforms with different inductance.

The voltage gain in DCM operation is

$$G_{DCM} = \frac{V_o}{V_i} = \frac{1}{2} + \frac{1}{2} \sqrt{1 + \frac{8D^2}{\tau}} \quad (21)$$

C. Operating Modes with Different Inductance

Assuming the inductance of the inductors is unequal, the operating modes of the converter are quite different with the situation when the inductance is equal. The following analysis is given on SH-SLC as an example, the operation principles of AH-SLC is similar. The CCM operation of SH-SLC is analyzed in the following. The possible situations are too excessive to analyze, in orderto simplify the analysis, assuming the ordering of the inductance is L1a < L1b < L2a < L2b. The key waveforms in CCM operation is shown in Fig. 8. The equivalent circuit is given in Fig. 9.

International Journal of Research
Available at https://edupediapublications.org/journals
p-ISSN: 2348-6848
e-ISSN: 2348-795X
Volume 03 Issue 13
September 2016

1) Mode 1[t0 − t1]: During this time interval, S1 and S2 are turned on. The equivalent circuit is shown in Fig. 9(a). The four inductors are charged in parallel by the power source. The voltage across the inductors can be expressed with equation (12).

2) Mode 2 [t1 − t2]: During this time interval, S1 and S2 are turned off. The equivalent circuit is shown in Fig. 9(b).

The inductors L1b, L2a, L2b are short-circuited. L1a is discharged to output. iL1a decreased with the rate (Vo − Vi)/L1a and iL1b, iL2a, iL2b remain unchanged. The voltage across the inductors is

$$\begin{cases} V_{L1a} = V_i - V_o \\ V_{L1b} = V_{L2a} = V_{L2b} = 0 \end{cases} \quad (22)$$

3) Mode 3 [t2 − t3]: During this time interval, S1 and S2 are turned off. The equivalent circuit is shown in Fig. 9(c).

During the time t2, iL1a(t2) = iL1b(t2), D1b is reversebiased, The inductors L2a, L2b are short-circuited. L1a and L1b are series connected and transfer the energy to output. iL1a, iL1b is decreased with the rate (Vo −Vi)/(L1a + L1b) and iL2a, iL2b remain unchanged. Thevoltage across the inductors is

$$\begin{cases} V_{L1a} = \frac{L_{1a}}{L_{1a}+L_{1b}}(V_i - V_o) \\ V_{L1b} = \frac{L_{1b}}{L_{1a}+L_{1b}}(V_i - V_o) \\ V_{L2a} = V_{L2b} = 0. \end{cases} \quad (23)$$

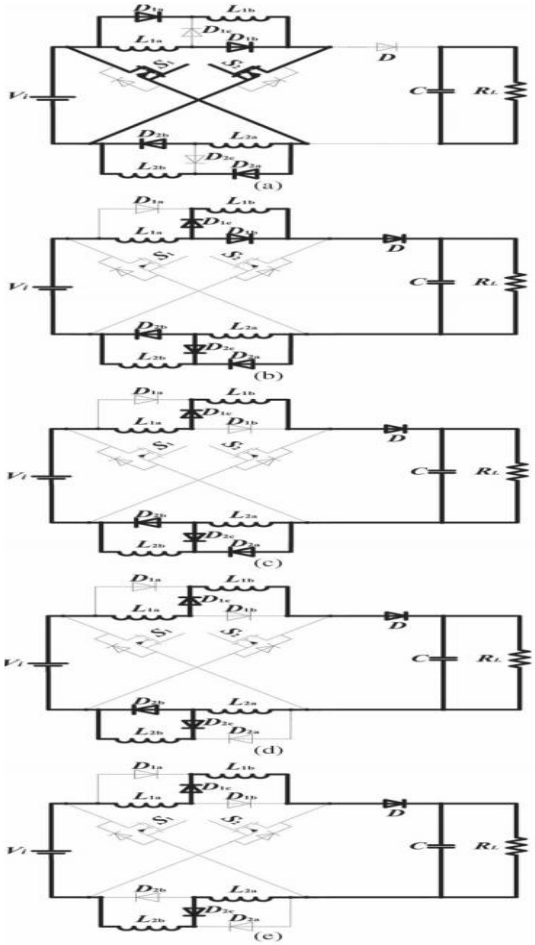

Fig. 9. Equivalent circuit of SH-SLC with different inductance.

4) Mode 4 [t3 − t4]: During this time interval, S1 and S2 are turned off. The equivalent circuit is shown in Fig. 9(d). During the time t3, iL1a(t3) = iL1b(t3) = iL2a(t3), D2a is reverse-biased, The inductor L2b is short-circuited. L1a, L1b, L2a are series connected and transfer the energy to output. iL1a, iL1b, iL2a is decreased with the rate (Vo − Vi)/(L1a + L1b + L2a) and iL2b remains unchanged. The voltage across the inductors is

$$\begin{cases} V_{L1a} = \frac{L_{1a}}{L_{1a}+L_{1b}+L_{2a}}(V_i - V_o) \\ V_{L1b} = \frac{L_{1b}}{L_{1a}+L_{1b}+L_{2a}}(V_i - V_o) \\ V_{L2a} = \frac{L_{2a}}{L_{1a}+L_{1b}+L_{2a}}(V_i - V_o) \\ V_{L2b} = 0. \end{cases} \quad (24)$$

5) Mode 5 [t4 − t5]:During this time interval, S1 and S2 are turned off. The current-flow path is shown in Fig. 9(e). During the time t4, iL1a(t4) = iL1b(t4) = iL2a(t4) = iL2b(t4), D2b is reverse-biased. L1a, L1b, L2a, L2b are series connected and discharged to output. iL1a, iL1b, iL2a, iL2b is decreased with the rate (Vo − Vi)/(L1a + L1b + L2a + L2b). The voltage across the inductors is

$$\begin{cases} V_{L1a} = \frac{L_{1a}}{L_{1a}+L_{1b}+L_{2a}+L_{2b}}(V_i - V_o) \\ V_{L1b} = \frac{L_{1b}}{L_{1a}+L_{1b}+L_{2a}+L_{2b}}(V_i - V_o) \\ V_{L2a} = \frac{L_{2a}}{L_{1a}+L_{1b}+L_{2a}+L_{2b}}(V_i - V_o) \\ V_{L2b} = \frac{L_{2b}}{L_{1a}+L_{1b}+L_{2a}+L_{2b}}(V_i - V_o) \end{cases} \quad (25)$$

Based on the voltage–second balancing of inductors, combining the equations (12), (22)–(25), the voltage gain in CCM operation with different inductance is

$$G'_{CCM} = \frac{V_o}{V_i} = \frac{1+3D}{1-D} \quad (26)$$

Compared with (15), the voltage gain is the same.

E. Magnetic Components Integration Consideration

In fact, all the inductors of the proposed topology with equal inductance share the same operation condition. As shown in Fig. 10, the inductors can be integrated into one magnetic core, which helps to reduce the size of magnetic components.

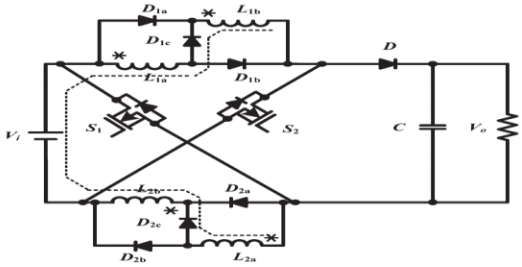

Fig. 10. Magnetic components integration.

International Journal of Research
Available at https://edupediapublications.org/journals
p-ISSN: 2348-6848
e-ISSN: 2348-795X
Volume 03 Issue 13
September 2016

IV.MATLAB/SIMULATION RESULTS

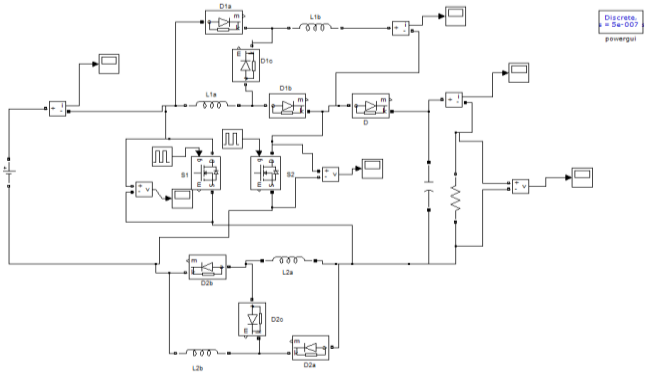

Fig.11.Matlab/Simulink model of hybrid switched inductor converters with open loop controller.

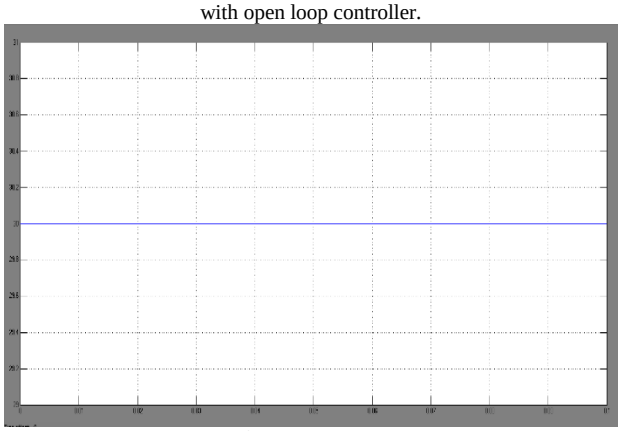

Fig.12.Input voltage of hybrid switched inductor converters.

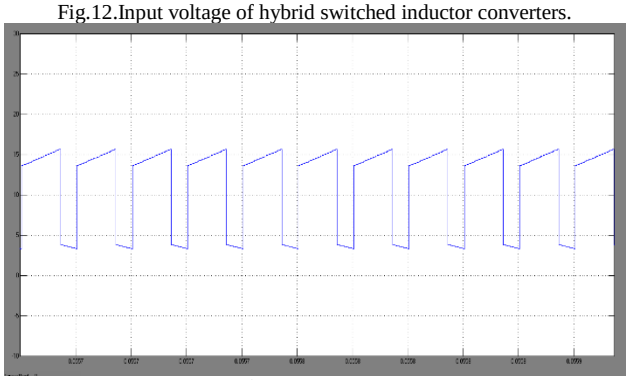

Fig.13.Input current of hybrid switched inductor converters.

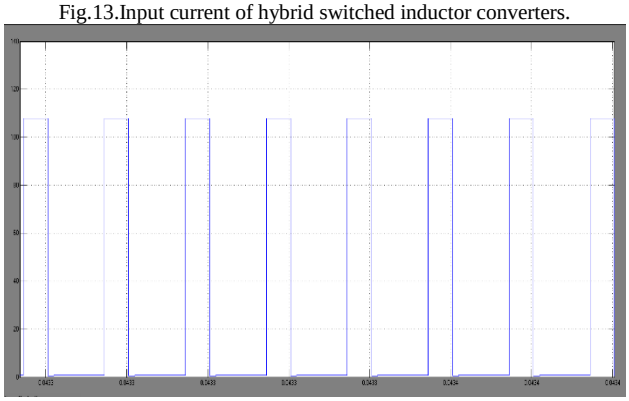

Fig.14.Switch Voltage (Vs1) converter.

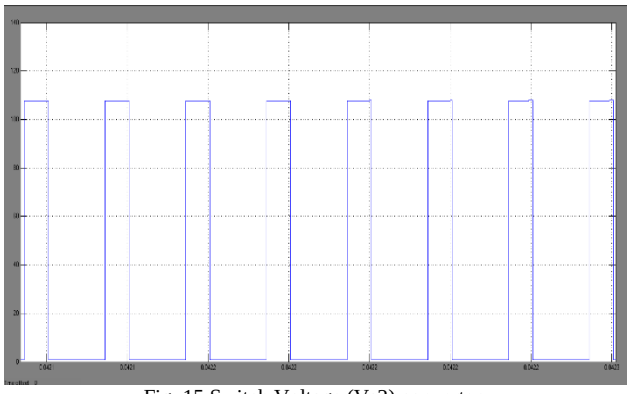

Fig .15.Switch Voltage (Vs2) converter.

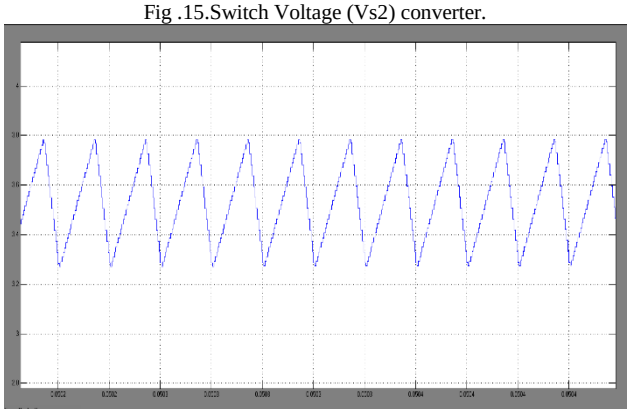

Fig.16.inductor Current.

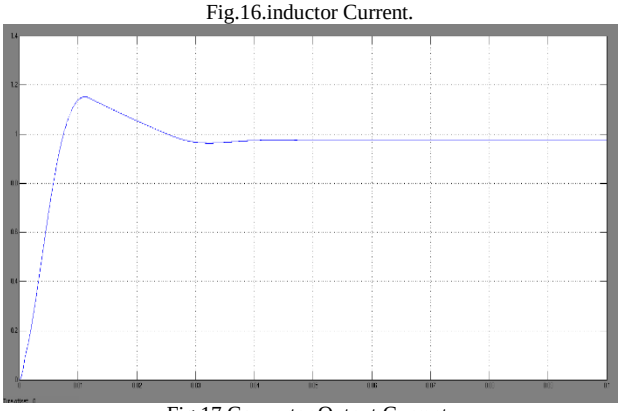

Fig.17.Converter Output Current.

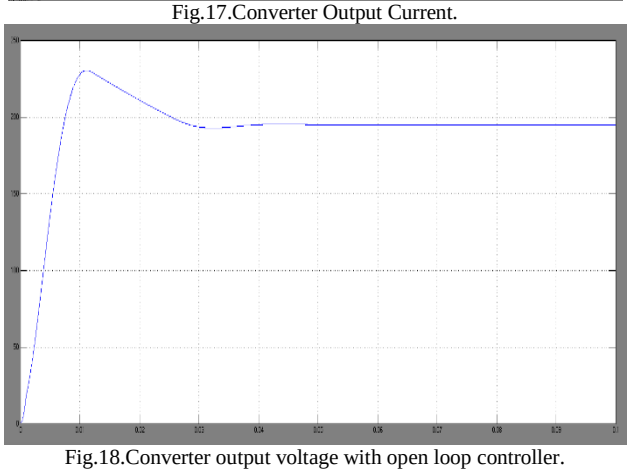

Fig.18.Converter output voltage with open loop controller.

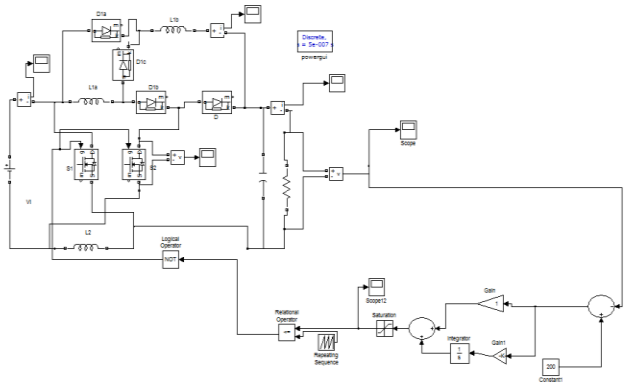

Fig.19.Matlab/Simulink model of hybrid switched inductor converters with closed loop controller.

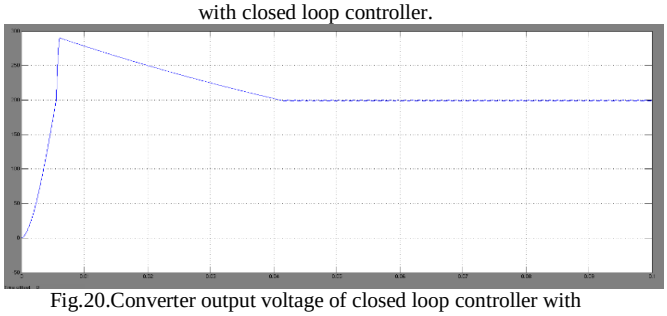

Fig.20.Converter output voltage of closed loop controller with references voltage is 200V.

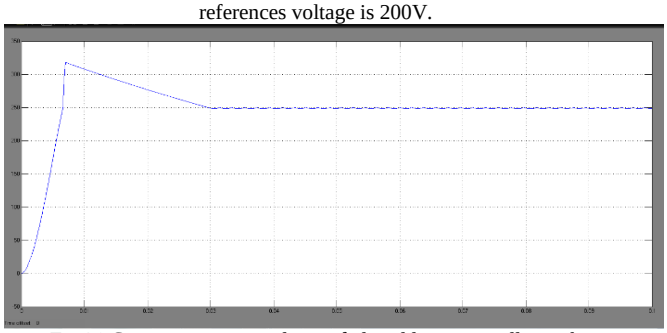

Fig.21.Converter output voltage of closed loop controller with references voltage is 250V.

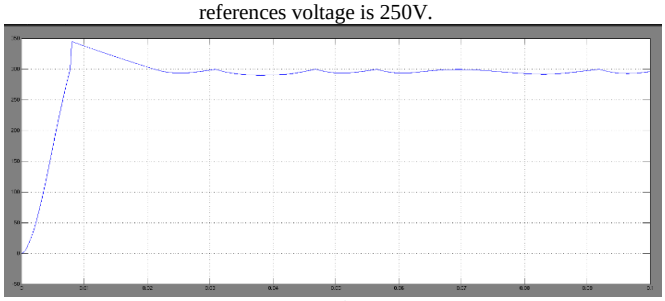

Fig.22.Converter output voltage of closed loop controller with references voltage is 300V.

V.CONCLUSION

The study of different converters has resulted in a new switching cell. The new switching cell combines the idea of two switching cells presented in two different papers. The insertion of new switching cell in conventional dc-dc converter has resulted in hybrid switch converter. The result of this new DC-to-DC converter is compared with other converters. The proposed converter has better advantages over conventional DC-to-DC converters with respect to high efficiency, high voltage conversion ratio and reduced switch voltage stress.A dc-dc converter family intended for fuel cell applications has been presented and analyzed. This family was developed by applying circuit structure modification with the fundamental idea of breaking the symmetry of traditional dc-dc converters.The structures of the proposed converters are very simple. This paper presents transformer less dc-dc converters with closed loop control to achieve high step-up voltage gain without an extremely high duty ratio. And a closed loop control strategy is adopted to avoid voltage drift problems.

REFERENCES

[1].Yu Tang, Member, IEEE, Dongjin Fu, Ting Wang, and Zhiwei Xu"Hybrid Switched-Inductor Converters for High Step-Up Conversion"IEEE Transactions on Industrial Electronics, Vol. 62, No. 3, March 2015.

[2] X. Wu, J. Zhang, X. Ye, and Z. Qian, "Analysis and derivations for a family ZVS converter based on a new active clamp ZVS cell," IEEE Trans. Ind. Electron., vol. 55, no. 2, pp. 773–781, Feb. 2008.

[3] R. G. Ganesan and M. Prabhakar, "Non-isolated high gain boost converter for photovoltaic applications," in Proc. IEEE ICPEC, 2013, pp. 277–280.

[4] L. S. Yang and T. J. Liang, "Analysis and implementation of a novel bidirectional DC-DC converter," IEEE Trans. Ind. Electron., vol. 59, no. 1, pp. 422–434, Jan. 2012.

[5] C. T. Pan and C. M. Lai, "A high-efficiency high step-up converter with low switch voltage stress for fuel-cell system applications," IEEE Trans. Ind. Electron., vol. 57, no. 6, pp. 1998–2006, Jun. 2010.

[6] H. M. Hsu and C. T. Chien, "Multiple turn ratios of on-chip transformer with four intertwining coils," IEEE Trans. Electron Devices, vol. 61, no. 1, pp. 44–47, Jan. 2014.

[7] X. Zhang et al., "A wide bandgap device-based isolated quasi-switchedcapacitor DC/DC converter," IEEE Trans. Power Electron., vol. 29, no. 5, pp. 2500–2510, May 2014.

[8] B. Gu, J. Dominic, J. S. Lai, Z. Zhao, and C. Liu, "High boost ratio hybrid transformer DC-DC converter for photovoltaic module applications," IEEE Trans. Power Electron., vol. 28, no. 4, pp. 2048–2058, Apr. 2013.

[9] H. S. Kim, J. W. Baek, M. H. Ryu, J. H. Kim, and J. H. Jung, "The high-efficiency isolated AC-DC converter using the three-phase interleaved LLC resonant converter employing the Y-connected rectifier," IEEE Trans. Power Electron., vol. 29, no. 8, pp. 4017–4028, Aug. 2014.

[10] M. Sarhangzadeh, S. H. Hosseini, M. B. B. Sharifian, and G. B. Gharehpetian, "Multiinput direct DC-AC converter with high-frequency link for clean power-generation systems," IEEE Trans. Power Electron., vol. 26, no. 6, pp. 1777–1789, Jun. 2011.

[11] P. H. Tseng, J. F. Chen, and Y. P. Hsieh, "A novel active clamp high step-up DC-DC converter with coupled-inductor for fuel cell system," in Proc. IEEE IFEEC, 2013, pp. 326–331.

[12] Y. H. Hu, W. D. Xiao, W. H. Li, and X. N. He, "Three-phase interleaved high-step-up converter with coupled-inductor-based voltage quadrupler," IET Power Electron., vol. 7, no. 7, pp. 1841–1849, Jul. 2014.

[13] Y. Zhao, W. H. Li, and X. N. He, "Single-phase improved active clamp coupled-inductor-based converter with extended voltage doubler cell,"IEEE Trans. Power Electron., vol. 27, no. 6, pp. 2869–2878, Jun. 2012.

[14] T. Meng, S. Yu, H. Q. Ben, and G. Wei, "A family of multilevel passive clamp circuits with coupled inductor suitable for single-phase isolatedFull-bridge boost PFC converter," IEEE Trans. Power Electron., vol. 29, no. 8, pp. 4348–4356, Aug. 2014.